MEASUREMENT OF THE ELECTRON CLOUD PROPERTIES BY MEANS OF A MULTI-STRIP DETECTOR IN THE CERN SPS

G. Arduini, P. Collier, B. Dehning, G. Ferioli, B. Henrist, L. Jensen, J.M. Jimenez, J.M. Laurent, G. Rumolo, K.Weiss, F. Zimmermann, CERN, Geneva, Switzerland

Abstract

Electron cloud effects presently limit the performances of the CERN SPS with LHC type beams [1] and are of concern for the LHC itself [2]. Electron multipacting in the SPS produces dramatic dynamic pressure increases and strong transverse instabilities [3]. In the LHC the electron cloud is expected to significantly increase the heat load in the cryogenics system. Estimates of these effects are based on computer simulations of the electron cloud build-up and of its spatial distribution in field free regions and in strong magnetic fields. The accuracy of such simulations is therefore a key issue for component design and for the definition of the operating strategies for the LHC. In 2001 a multi-strip detector has been installed in the SPS to study the electron cloud and to provide experimental data to validate the models and to better constrain their input parameters. After a description of the monitor characteristics and of its associated electronics an overview of its performance and of the results of the measurements conducted with different proton beam parameters are presented. The measurements are compared with simulation results. Possible monitor upgrades are also discussed.

1 INTRODUCTION

Electron cloud effects have been observed at CERN since 1999 when LHC-type beams were injected for the first time in the SPS. In 2001 electron cloud effects were visible in the arcs for bunch intensities $I_{bunch} > 0.3 \times 10^{11}$ p and in the straight sections for $I_{bunch} > 0.6 \times 10^{11}$ p. Various codes have been developed to simulate the electron-cloud build-up [4] with the aim of understanding the observations in the SPS and of quantifying the additional heat load on the LHC cryogenic system due to the electron cloud [5].

In the dipoles electrons are concentrated in two stripes, symmetrically positioned with respect to the beam [4], as a combined effect of the electron energy distribution and of the Secondary Emission Yield (SEY) energy dependence. At the position of each stripe the electron energy gain corresponds to the value of the energy for which SEY is maximum. In the SPS, for $I_{bunch} < 0.5 \times 10^{11}$p, the two stripes collapse in one because of the lower energy gained by the electrons. A third central stripe is predicted by simulations for $I_{bunch} \sim 10^{11}$p. The knowledge of the position of the stripes as a function of I_{bunch} is of primary importance for the LHC because of the presence of pumping slots. The superimposition of the electron stripes with the pumping slots could either imply a dramatic increase of the heat load deposited on the cold-bore at 1.9 K, or a local suppression of the multipacting if the pumping slots act as electron traps [5].

In order to benchmark the simulation programs and provide constraints for the input parameters a test bench to measure the electron cloud properties in a dipole magnetic field of variable strength was designed and installed in the SPS in 2001.

2 EXPERIMENTAL SET-UP

2.1 Magnetic field

Four large aperture (~ 200x200 mm) dipole magnets providing vertical magnetic fields are powered in series by a bi-polar power converter and they are arranged in a wiggler-like configuration (↑↓↓↑). The 'wiggler' produces only a local orbit distortion. The maximum magnetic field is 0.244 T (for comparison the magnetic field at injection in the SPS in 0.12 T) and it can be reverted in few seconds.

2.2 Detector and associated electronics

The detector consists of 16 copper strips, each 2 mm thick and 300 mm long, deposited on a MACOR™ substrate with a 2.5 mm pitch. Two larger strips are deposited on both sides for grounding purposes (Fig. 1).

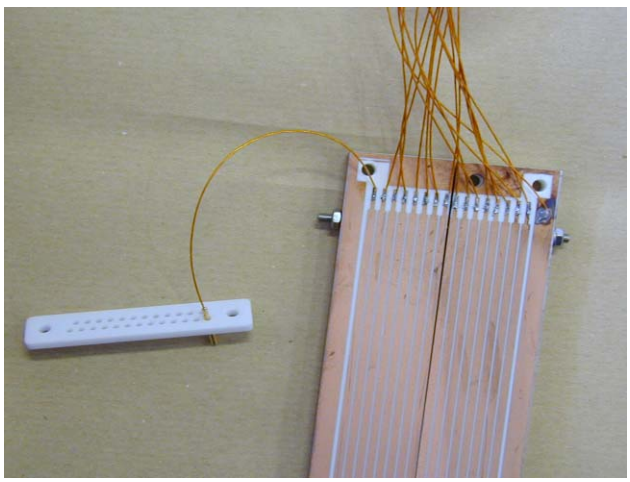

Figure 1: The multi-strip detector.

In order to avoid any perturbation of the multipacting process the monitor is installed under vacuum in an antechamber located beneath a standard stainless steel main bend (MBA) vacuum chamber. A series of holes (2 mm diameter and 6 mm pitch) is drilled in the vacuum chamber surface in front of the detector in all its length (Fig. 2) providing a geometric transparency (i.e. the ratio

of the total surface of the holes to the surface of the monitor) of 7.5 %. The holes are arranged in rows inclined with respect to the beam direction in order to avoid any systematic dependence of the signal generated by an electron stripe on its position. The residual modulation of the electron signal as a function of the stripe position was estimated to be ± 10 % for the chosen configuration, assuming an electron stripe width of 2 mm. The estimation was based only on geometrical considerations. The transparency has been chosen as the minimum permitting to collect a detectable signal on each strip on the basis of the electron-cloud density estimated from simulations and of the sensitivity of the chosen electronics.

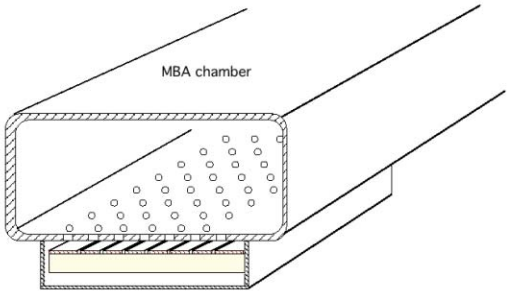

Fig. 2: Detector assembly in the MBA chamber.

An existing 8-bit resolution design [6] has been chosen for the acquisition electronics. This solution is already used for the measurement of the extraction spill in the transfer lines by means of secondary emission monitors. The integration time can be varied from 1 to several ms (typical values during the measurements were ranging from 1 to 5 ms) and a maximum gain of 20 can be applied. The minimum detectable current in a strip is 4 nA for the maximum gain while the saturation current for the minimum gain is 20 μA. The expected electron current per strip was of the order of a μA per LHC bunch train.

In order to avoid low frequency noise the vacuum chamber has been equipped with enamelled flanges, the conduction of high frequency components being guaranteed by condensers installed in parallel to the collars. The two external strips of the detector are connected to ground at the electronics crate in a surface building.

3 MEASUREMENTS

The detector provided very rapidly good quality signals in the presence of LHC-type beam and magnetic field. The nature of the observed signal as electron cloud was inferred from the following observations:

- No signal was observed without beam.
- No signal was observed with fixed target beam* at injection, as expected from simulations.
- The signal was spatially correlated with the beam position when this was varied.
- The threshold I_{bunch} for the appearance of the signal was comparable with that for the dynamic pressure rises observed in the arcs.
- No signal was detected without magnetic field, in agreement with the observation that pressure increments were observed only in the arcs.

3.1 Magnetic field dependence

The dependence of the electron cloud signal on the magnetic field has been studied in detail for different I_{bunch} in order to understand the role of the magnetic field in the electron cloud build-up. It has been observed that decreasing the magnetic field the transverse size of the electron cloud distribution increases and the total electron cloud signal (i.e. the sum of the signals in all the 16 channels) grows rapidly until it drops abruptly for magnetic fields B lower than few 10^{-3} T (Fig. 3).

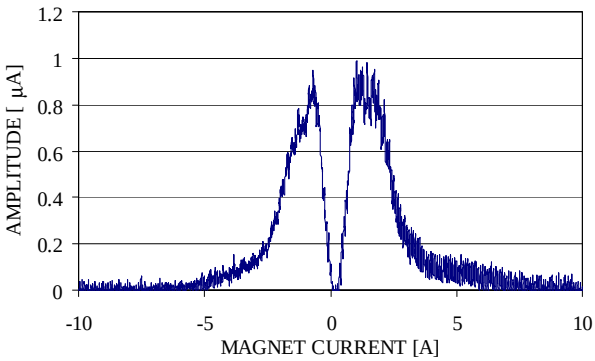

Fig. 3: Dependence on the dipole current.

Electrons in a dipole magnetic field do not gain significant transverse energy (w.r.t. the field direction), therefore they have transverse energies in the range 1-10 eV. For a 10 eV electron the cyclotron radius increases from 0.04 mm at B=0.244 T to 11 mm at B=10^{-3} T. At the highest field the holes in the vacuum chamber represent a significant perturbation to multipacting while at low field the holes are not distinguished by the spiralling electrons. This might explain the growth in the electron cloud signal observed when the magnetic field is reduced. For B=10^{-3} T the cyclotron period becomes comparable to the bunch spacing and the motion of the electrons is comparable to that in a field free region. Electron cloud simulations foresee higher threshold intensities for field free regions [4] and could explain the disappearance of the electron cloud signal at low fields.

3.2 Dependence on bunch intensity

The determination of the dependence of the electron cloud distribution on I_{bunch} was the main motivation for the design of the strip detector. Fig. 4 shows the electron cloud transverse distribution for LHC-type beams for two

* The fixed target beam consists of 2 trains each filling 5/11 of the SPS ring and separated by a gap of 1/22 of the SPS ring. The revolution period is ~ 23 μs. Each train consists of 2100 bunches with a bunch spacing of 5 ns. I_{bunch} ~ a few 10^9 p.

different intensities. The observations qualitatively confirm the results of the simulations: for $I_{bunch} < 0.5 \times 10^{11}$ p a single stripe is observed and for $I_{bunch} > 0.5 \times 10^{11}$ p/bunch two stripes appear. Recent measurements have also confirmed the appearance of a third stripe for $I_{bunch} \sim 1.1 \times 10^{11}$ p. A sensible discrepancy remains between the measured strip separation and the estimated one, the latter being twice as large as the measured one. This might require reconsidering the parametrization of the SEY used in the simulations and based on measurements on copper samples carried out at CERN [7]. As a result of this measurement the location and design of the pumping slots of the beam screen are being revised.

a)

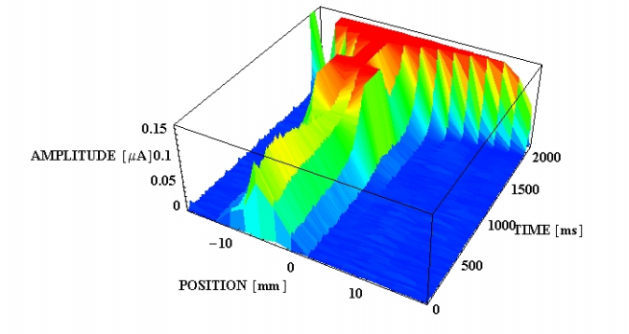

b)

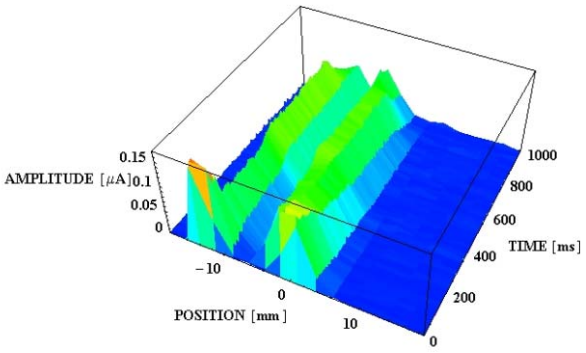

Fig. 4: Electron cloud signal vs. time. a) $I_{bunch} \sim 0.5 \times 10^{11}$ p. The magnetic field is reduced from 0.244 T down to 0 in 2 s. b) $I_{bunch} \sim 0.6 \times 10^{11}$ p.

3.3 Electron Cloud for the Fixed Target Beam

Data taken with the strip detector evidenced electron cloud build-up with the fixed target beam during acceleration. The maximum signal does not appear at transition, when bunches have the minimum length, but later in the ramp when the beam size is shrinking. This suggests that not only bunch length but also transverse beam size is affecting the electron-cloud build-up.

3.4 Effect of electron bombardment

Beam induced electron bombardment is expected to modify the SEY of the walls of the vacuum chamber and therefore to increase the threshold for multipacting. Because of the transverse distribution of the electron cloud it is reasonable to imagine that the conditioning effect is not uniform. Measurements performed both with LHC and fixed target beams after several tens of hours of operation with Fixed Target and LHC beams have confirmed this hypothesis. Fig. 5 shows the transverse electron cloud distribution as a function of the horizontal beam position that was varied by creating a local bump. A region with suppressed multipacting is visible in the centre of the monitor.

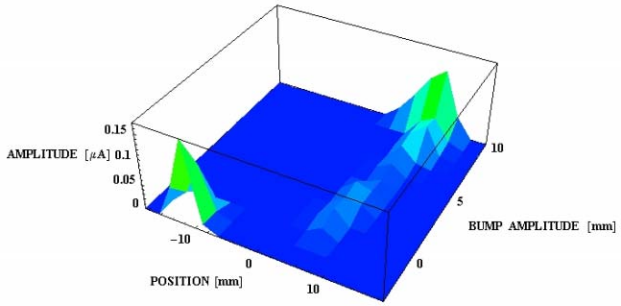

Fig. 5: Electron cloud signal vs. horizontal beam position.

4 CONCLUSIONS

An innovative monitor for the measurement of the transverse properties of the electron cloud has been installed in the SPS in 2001. Observations are in qualitative and quantitative agreement with simulations with the exception of the distance between the electron stripes. This is overestimated by simulations. The measurements permitted to achieve additional insight of the electron cloud build-up and to provide valuable input for the LHC beam screen design. During the 2001-2002 shutdown a new monitor, of similar design but with improved resolution, has been installed and preliminary measurements have been performed confirming the appearance of a third stripe for $I_{bunch} \sim 1 \times 10^{11}$ p.

ACKNOWLEDGEMENTS

We would like to thank all the equipment groups involved in the design and installation of the detector, in particular: A. Beuret, J. Ramillon, M. Royer, D. Smekens, A. Spinks.

REFERENCES

[1] G. Arduini et al., 'Status of the LHC Beam in the CERN SPS', these Proceedings.
[2] R. Schmidt, 'Status of the LHC', these Proceedings.
[3] K. Cornelis et al., 'Electron Cloud Instability in the SPS', these Proceedings.
[4] G. Rumolo, F .Zimmermann, 'E-Cloud Simulations: Build-up and Related Effects', ECLOUD'02, (http://slap.cern.ch/ collective/ecloud02/).
[5] F. Zimmermann, 'Electron-Cloud effects in the LHC', ECLOUD'02.
[6] G. Buur and G. Ferioli, SL Note 94-01 BI.
[7] N. Hilleret, 'An empirical fit to the true electron energy distribution', unpublished draft dated 23/10/2001.